

Development of Poly(propylene) Superhydrophobic Surfaces by Functionalised TiO₂ Nanoparticles: Effect of Solvents and Dipping Times

Gabriela Ramos Chagas,* Daniel Eduardo Weibel

Summary: We present a simple strategy for the fabrication of poly(propylene) (PP) superhydrophobic surfaces, i.e., surfaces that show water contact angle (WCA) $\geq 150^\circ$ after a simple dipping process. Injection-moulded PP samples were coated with titanium dioxide nanoparticles previously functionalised with trimethoxy propyl silane. Water, ethanol or xylene were used as solvents in the nanoparticles' suspensions. The prepared superhydrophobic surfaces were characterised by WCA, FTIR-ATR, SEM and profilometry measurements. PP coated samples showed very low wettability, with WCAs higher than 150° when xylene was used as a solvent. The combination of increasing the surface roughness via dipping coating process plus the low surface tension of the coating produced the final superhydrophobic PP substrates.

Keywords: nanoparticles; poly(propylene); silane; superhydrophobicity; titanium dioxide

Introduction

Superhydrophobic surfaces have recently attracted researchers' attention due to their self-cleaning, anti-contamination, anti-sticking and anti-corrosion properties, which means they have many potential industrial applications.^[1–4] To be considered superhydrophobic, a material must have a water contact angle (WCA) between a water drop and the materials' surface of equal or greater to 150° . The wettability is directly related to two properties: surface energy, and roughness.^[4–9] Surface energy depends on chemical composition, and materials with low surface energy have high WCAs. These surfaces are considered hydrophobic. Rough surfaces or those with microstructures can also increase the WCA of the material; as a consequence of the combination of roughness with a low surface energy coating, a superhydrophobic state can be reached.^[4–13]

Superhydrophobicity is found, for example, in the lotus leaf, which has micro- and nano-

structured leaves that hinder the fixation of water droplets. This property causes droplets to contract into spherical shapes and to slide on the surface. This phenomenon is called the 'lotus effect'.^[4–7,11,13] Studies showed that the surface of the lotus leaf has a WCA of approximately 161° , with a hydrophobic wax nanocrystal microstructure.^[4] Because of this, lotus leaves can be kept clean and free from any contamination, even when the leaf is surrounded by muddy water. Many others leaf examples exist, such as petal leaves,^[14,15] lupin leaves, taro (*Colocasia esculenta*) leaves, India canna (*Canna generalis bailey*) leaves,^[4,7,13] and many others. All of these leaves have superhydrophobic properties. There are also other examples in nature in animals and insects, such as the gecko foot^[16–18] and the wings of some butterflies.^[4,11] Learning from nature has long been a source of bio-inspiration for scientists and engineers and in the last decade researches are trying to artificially create those properties using many types of materials: polymers,^[19–23] wood,^[24,25] metals,^[26–28] paper,^[29] textiles,^[30–33] and others.

Nanoparticles (NPs) have often been used in the preparation of superhydrophobic surfaces because they provide an easy way

Laboratory of Photochemistry and Surfaces, Chemical Institute, Universidade Federal do Rio Grande do Sul, Porto Alegre, RS, Brazil
E-mail: gabrielarchagas@hotmail.com

to create a nano-micro structured surface via the formation of clusters or aggregates on surfaces. These nano-micro structures increase the roughness of the material and thus increase the WCA.^[5,6,19,34,35] Titanium dioxide (TiO₂) and silicon dioxide (SiO₂) are metallic oxide semiconductors that have been widely employed to modify and confer specific surface properties, such as increasing the surface wettability. They also show great chemical and thermal stability compared to organic materials.^[19,34,35] TiO₂ is a very important material and can be used in many kinds of industrial applications such as solar cells, photocatalysis, photovoltaic devices and pigments, and it is one of the most widely-used compounds in developing reversible wettability.^[35–37] Ramanathan *et al.*^[38,39] prepared superhydrophobic surfaces using TiO₂ NPs on glass and metallic substrates, thus increasing the WCA between the substrate and the water drop. They used an aqueous and non-aqueous solvent to prepare the coating and observed different contact angle hysteresis and liquid-solid adhesion. Hou *et al.*^[35] obtained surfaces with reversible superhydrophobicity-superhydrophilicity wettability properties through a simple photochemistry treatment using hydrophilic TiO₂ NPs on polystyrene surfaces. Contreras *et al.*^[40] developed permanent polymeric superhydrophobic surfaces that were dependent on the hysteresis of the NP concentration and surface chemistry.

Due to the increased use of polymers in many industrial applications, this work aims to improve the surface properties of poly(propylene) (PP) by surface modification using TiO₂ NPs, functionalised with a short alkyl chain silane (trimethoxy propyl silane). The preparation of PP surfaces was carried out by a simple dip-coating method, using suspensions of TiO₂ NPs in several solvents and different dipping times.

Experimental Part

Sample Preparation

Polymer samples (BRASKEM-H 301) were processed by injection moulding,

cleaned in an ultrasonic bath with a sequence of solvents for removing organic residues, and then dried at room temperature. The final PP substrates were cut into sticks of size 1 cm x 1 cm. Trimethoxy propyl silane (TMPSi) of 97% purity was obtained from Sigma Aldrich. Xylene (mixture of isomers) and ethanol were purchased from Merck (Brazil). TiO₂ NPs obtained from Degussa Corporation: AEROXIDE® TiO₂-P25 were functionalised using a previously published procedure.^[41] Briefly, NPs with a concentration of 0.5% or 1.0% (% w/v) were immersed in suspensions containing a solvent/TMPSi solution ratio of 95/5% (v/v). The suspension was maintained in an ultrasonic bath for a few hours and heated to the desired temperature before PP dipping. PP samples were dipped in the above suspensions for 1, 5, 10 or 15 seconds. For ethanol and water solvents, the suspensions were kept at 50 °C due to their low boiling points of 78 °C and 100 °C, respectively. Higher temperatures can be used with xylene (boiling point 137–140 °C)^[42] and so xylene suspensions were heated to 130 °C for the sample preparation. Finally, the treated PP samples were dried at 100 °C for 2 hours.

Characterization of the Samples

Static WCA was measured at ambient temperature using a drop of deionized water (4 µL) by gently depositing it on the substrate using a micro syringe. The images were captured using the “Drop Shape Analysis System”, Kruss DSA 30 system. For each sample series, the final measurement was calculated from an average of five samples. FTIR-ATR (Alpha-P model, Bruker) spectra of the samples were obtained with a spectral resolution of 4 cm⁻¹. Morphology of the surfaces was observed by scanning electron microscopy (SEM), using EVO50-Carl Zeiss equipment and an electron acceleration of 10 kV. Profilometry analyses were carried out using Ambios XP-2 equipment with a stylus of 2.5 mm ratio. The square mean of the surface roughness (R_q) was calculated from the roughness profile.

Results and Discussion

WCAs of PP samples dipped in 1.0% functionalised TiO_2 NP suspensions in different solvents were measured (Figure 1). The WCA results obtained showed the different wettability of the final nanocoating.

The data presented in Figure 1 shows a strong dependence on the solvent used to prepare the TiO_2 functionalised suspension. When PP sticks were dipped in water suspensions, the WCA did not achieve the superhydrophobicity state, and when an ethanol suspension was used, the WCA increased to 141.8° . PP sticks were dipped in water or ethanol suspensions at a temperature of 50°C , due to the higher vapour pressure of these solvents; they did not achieve superhydrophobicity. However, when xylene was used as a solvent to prepare the suspension, the treated PP samples achieved a superhydrophobic state, with a WCA of 158.1° . The dipping temperature in the xylene suspension was closer to the softening temperature of PP (152.5°C), which enabled a slight opening of the polymer chains and provided better interaction of the functionalised TiO_2 NPs with the PP substrate. Additionally, PP is relatively soluble in xylene solvent, depending on the temperature, hence a few PP layers may partially dissolve on the surface region allowing for the anchoring of the

TiO_2 NPs more easily when the PP stick is removed from the suspension and the solvent is rapidly evaporated. The rapid cool down and simultaneous high evaporation rate of the xylene solvent leaves a surface with higher degree of modification than by using water or ethanol as solvents. SEM images presented in Figure 2 show the results of the dynamic dipping process described above.

The untreated PP substrate showed a smooth surface without the presence of any clusters or agglomerates (Figure 2a). However, when PP substrates were dipped in water or ethanol suspensions (Figure 2b, c) the formation of clusters and aggregates on the polymer surface were seen after the dip coating process, increasing the roughness of the surface and therefore the hydrophobicity. Water and ethanol solvents did not produce an appreciable dissolution of the PP surface, leaving many open regions of untreated PP that led to a final WCA lower than 150° . TiO_2 NPs formed aggregates on the PP surfaces when water or ethanol suspensions were used, which is similar to results observed in our previous publications on glass and silicon substrates.^[38,39]

In contrast, Figure 2(d) shows the results seen after xylene suspension dipping. The image shows the formation of clusters and aggregates together with a high dissolution of the PP matrix. The dipping in xylene

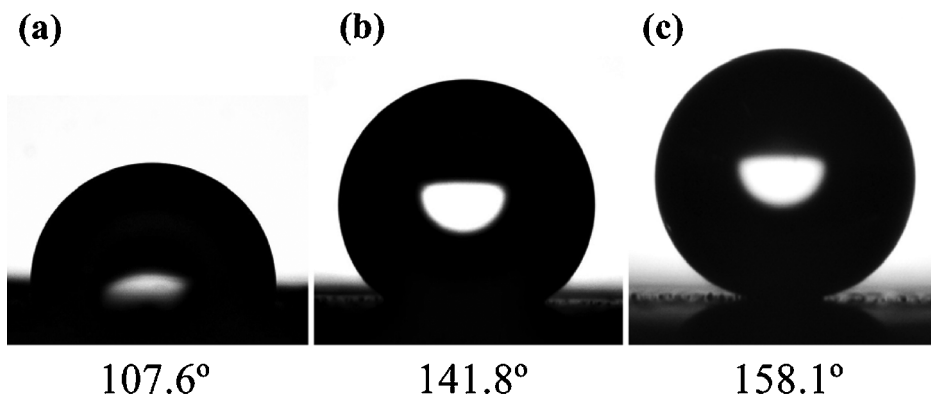


Figure 1.

Water drop images and contact angles of the PP surfaces after 5 seconds dipping in: (a) water, (b) ethanol and (c) xylene suspensions containing 1.0% of functionalised TiO_2 NPs.

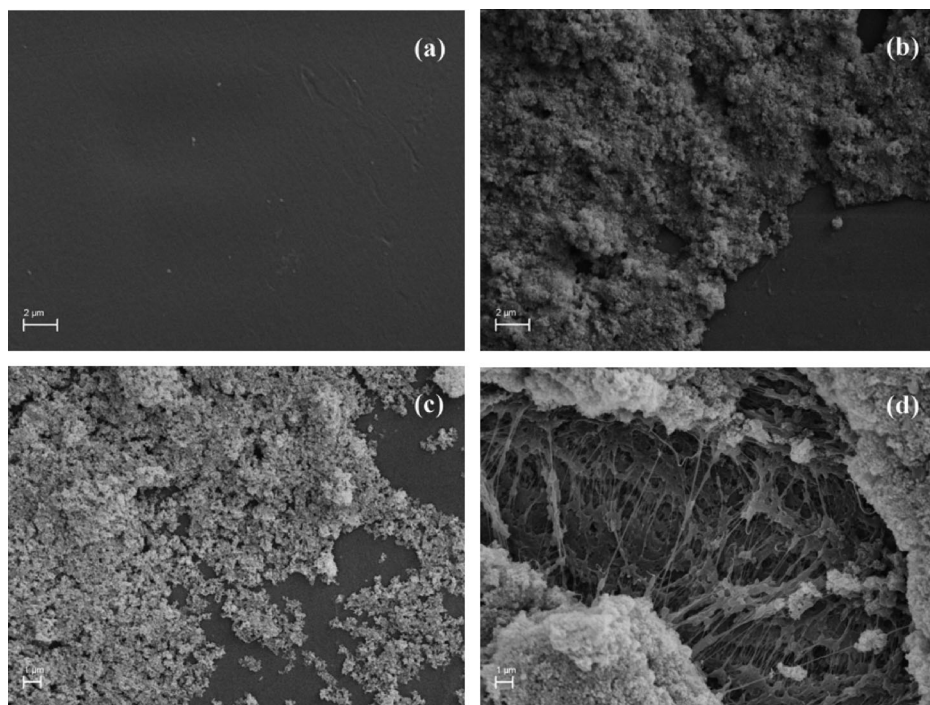


Figure 2.

SEM images of untreated PP samples (a), PP substrates after being dipped in water (b), ethanol (c), and xylene (d) suspensions with 1.0% of TiO_2 NPs and TMPSi for five seconds.

suspension and the high evaporation rate of the xylene solvent induced a large morphological change on the polymer surface, thus changing the roughness of the surface.

Figure 3 shows the FTIR-ATR spectra of PP substrates dipped in water, ethanol and xylene suspensions. From Figure 3, characteristic $-\text{OH}$ group signals from 3300 to 3000 cm^{-1} can be seen, only after water and ethanol dipping, showing that these polar solvents did not allow total functionalization of the TiO_2 NPs and therefore the PP substrates did not reach a superhydrophobic state. To support this interpretation, the $\text{Si}-\text{O}-\text{C}$ signal (ring link)^[43] at 1062 cm^{-1} and $\text{Si}-\text{O}-\text{Si}$ linkage at 1031 cm^{-1} were compared. In water and ethanol suspensions, the FTIR-ATR spectra showed a very strong increase in intensity when compared to the xylene suspension. This showed that the concentration of $\text{Si}-\text{O}-\text{Si}$ bonding (siloxanes) is high on the surface of water and ethanol

solvents and is mainly in the form of a ring link structure due to the hydrolysis and condensation reactions of TMPSi in polar solvents.^[44] Additionally, in Figure 3, the characteristic band of $\text{Ti}-\text{O}$ at approximately 455 cm^{-1} is more intense when ethanol and xylene suspensions are used compared to a water suspension. This difference supports the presence of a high rate of hydrolysis and condensation reactions of TMPSi in water.

The effect of dipping time of the PP sticks in the xylene suspension and the TiO_2 NPs concentrations was investigated and the results are summarised in Table 1. The treated PP substrates prepared in the present work showed relatively high hysteresis. In a previous study it was shown that self-cleaning conditions can only be obtained when the concentration of TiO_2 NPs was higher than 1.5%.^[40]

Table 1 shows that PP substrates coated with 0.5% (v/v) functionalised TiO_2 NPs

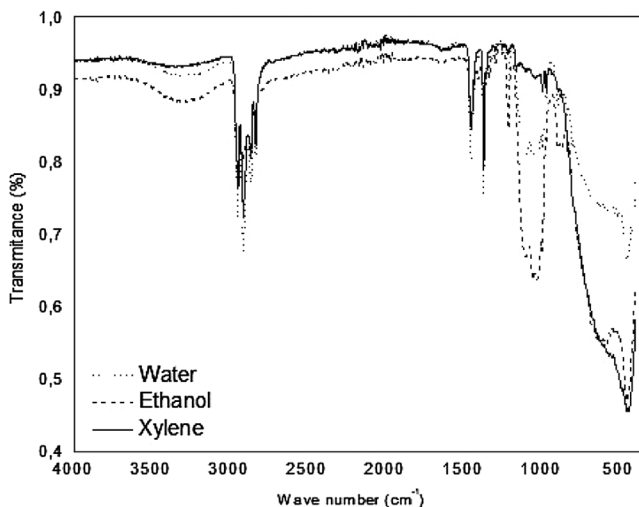


Figure 3.

FTIR-ATR spectra of functionalised PP sticks dipped in water, ethanol and xylene suspensions with TMPSi and 1.0% of TiO₂ NPs. Dipping time: 5 seconds.

reached a superhydrophobic state only at short dip times (1 and 5 seconds). After 10 seconds of dipping in the hot xylene suspensions, the final PP substrate lost the superhydrophobic state and showed a higher heterogeneity, as measured by the standard deviation (see Table 1). A higher dissolution rate of the PP substrate at longer dipping times may have meant that a different morphology was obtained compared to that showed in Figure 2d, and therefore a superhydrophobic state was not obtained. On the contrary, when the substrates were dipped in 1.0% (v/v) functionalised TiO₂ NPs, the final PP surface showed a continuous increase in

WCA, reaching a superhydrophobic state in almost 1 second of dipping (see Table 1). Except for the shortest dipping time used, all of the samples appeared more homogenous (lower standard deviations). The SEM images shown in Figure 4 show that at very short dipping times (Figure 4a) there is no important polymer dissolution, and mainly clusters and aggregates are formed after the fast evaporation of xylene. When the time increased, a clear opening of the PP surface was observed (Figure 4b). Longer dipping times may lead to a higher rate of PP dissolution with more homogenous trapping of TiO₂ NPs when the solvent evaporates after the dipping process.

FTIR-ATR analysis of PP substrates dipped in functionalised TiO₂ NPs with TMPSi in xylene solvent are shown in Figure 5. When the concentration of TiO₂ NPs in the suspension increased, a proportional increase was observed in the bands assigned to Ti—O (441.1 cm⁻¹) on the coated PP sticks, indicating the presence of a thicker nanocoating. On the contrary, the characteristic bands of the polymer C—H at 2915 cm⁻¹ and C—C at 1363 and 1460 cm⁻¹ decreased in intensity with

Table 1.

WCA of untreated and coated PP sticks after dipping in 0.5% or 1.0% (v/v) of functionalised TiO₂ NPs in xylene/TMPSi suspension. Dipping time: 5 seconds.

Dipping time	WCA (degrees)	
	0.5% TiO ₂ NPs	1.0% TiO ₂ NPs
PP untreated	104 ± 1	104 ± 1
1 second	151 ± 1	148 ± 7
5 seconds	152 ± 1	153 ± 1
10 seconds	146 ± 5	152 ± 3
15 seconds	148 ± 6	154 ± 5

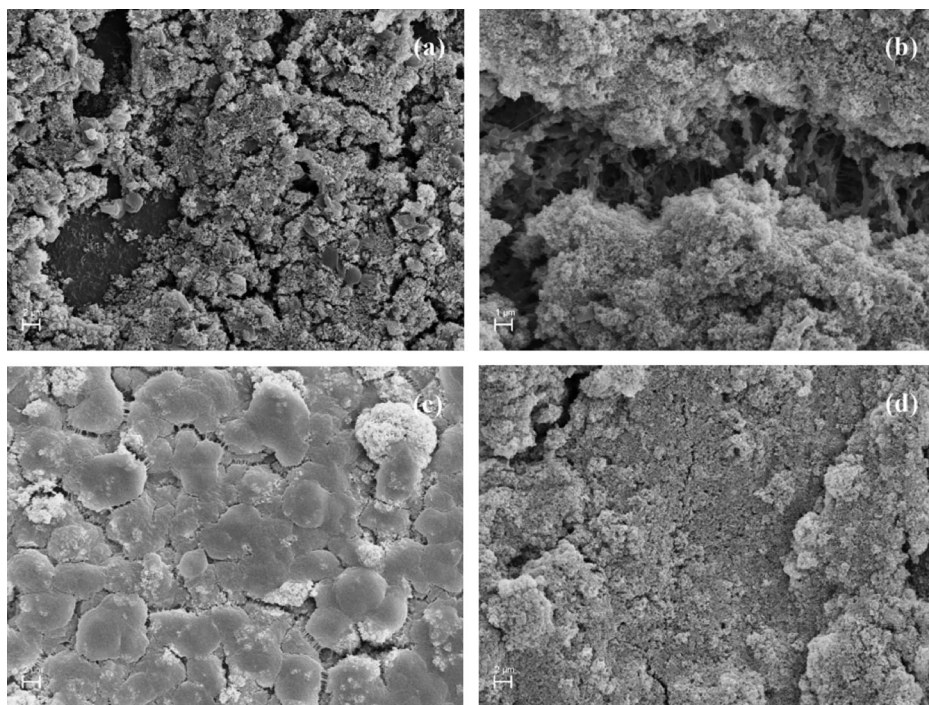


Figure 4.

SEM images of PP samples after being dipped in 1.0% functionalised TiO_2 NPs with TMPSi in xylene solvent. Dipped time: 1 s (a), 5 s (b), 10 s (c) and 15 s (d).

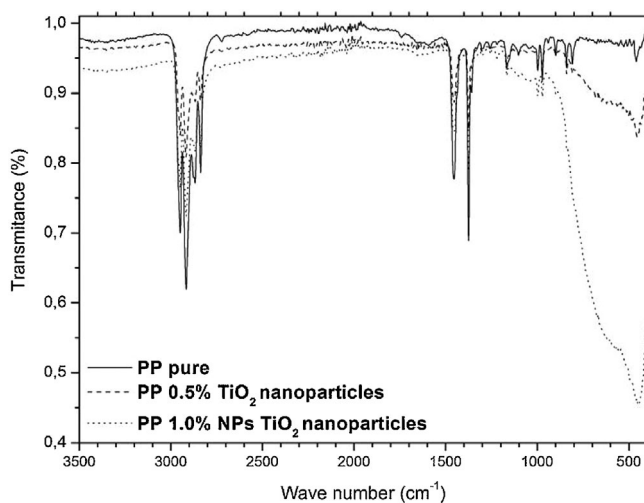


Figure 5.

FTIR-ATR spectra of untreated and dipped PP sticks in xylene suspensions containing different concentrations of TMPSi-functionalised TiO_2 NPs. Dipping time: 5 seconds.

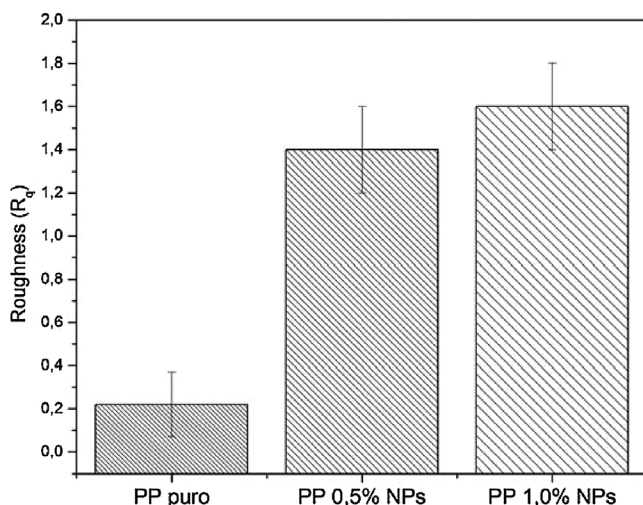


Figure 6.

R_q results of untreated and coated PP with 0.5% and 1.0% functionalised TiO_2 NPs in xylene/TMPSi suspension. Dipping time: 5 seconds.

increasing TiO_2 NP concentration. Both FTIR-ATR results confirmed a proportional increase of the nanocoating when the functionalised TiO_2 NPs concentration increased.

To correlate the differences observed in the WCA measurements for untreated and coated PP samples, profilometry measurements were carried out for samples that were dipped for 5 seconds. Figure 6 shows the profilometry results when the PP sticks were dipped in xylene solutions with 0.5% and 1.0% of TiO_2 NPs.

The increase in roughness of the samples compared with untreated PP after they were coated with functionalised TiO_2 NPs is evident in Figure 6; this explains the superhydrophobic properties obtained in the treated PP samples.

Conclusion

In summary, we have presented a simple method for preparing a superhydrophobic PP surface in one step, by using TiO_2 NPs functionalised with TMPSi. The nanocoating changed the natural hydrophobic properties of the PP substrates to superhydrophobic only when xylene was used as a solvent. It

was shown that a very short dipping time is enough for obtaining a superhydrophobic surface. SEM images and profilometry measurements confirmed that the combination of partial solubility of the PP and inclusion of TiO_2 NPs with cluster formation in the surface region provided the necessary roughness required for a PP superhydrophobic surface to be obtained.

- [1] Z. Xue, M. Liu, L. Jiang, *J. Polym. Sci., Part B: Polym. Phys.* **2012**, 50(17), 1209.
- [2] E. Celia, T. Darmanin, E. T. de Givenchy, S. Amigoni, F. Guittard, *J. Colloid Interface Sci.* **2013**, 402(0), 1.
- [3] X.-M. Li, D. Reinhoudt, M. Crego-Calama, *Chem. Soc. Rev.* **2007**, 36(8), 1350.
- [4] Y. Y. Yan, N. Gao, W. Barthlott, *Adv. Colloid Interface Sci.* **2011**, 169(2), 80.
- [5] C.-H. Xue, S.-T. Jia, J. Zhang, J.-Z. Ma, *Sci. Technol. Adv. Mater.* **2010**, 11(3), 033002.
- [6] X.-M. Li, D. Reinhoudt, M. Crego-Calama, *Chem. Soc. Rev.* **2007**, 36(8), 1350.
- [7] E. Celia, T. Darmanin, E. Taffin de Givenchy, S. Amigoni, F. Guittard, *J. Colloid Interface Sci.* **2013**, 402(0), 1.
- [8] D. E. Weibel, A. F. Michels, A. F. Feil, L. V. Amaral, Sr. S. Teixeira, F. V. Horowitz, *J. Phys. Chem. C* **2010**, 114(31), 13219.
- [9] C.-H. Xue, J.-Z. Ma, *J. Mater. Chem. A* **2013**, 1(13), 4146.
- [10] M. Ma, R. M. Hill, *Curr. Opin. Colloid Interface Sci.* **2006**, 11(4), 193.

- [11] M. A. Samaha, H. V. Tafreshi, M. Gad-el-Hak, C. R. Mec. **2012**, 340(1–2), 18–34.
- [12] D. E. Weibel, A. F. Michels, F. Horowitz, R. da Silva Cavalheiro, G. V. da Silva Mota, *Thin Solid Films* **2009**, 517(18), 5489–5495.
- [13] N. J. Shirtcliffe, G. McHale, S. Atherton, M. I. Newton, *Adv. Colloid Interface Sci.* **2010**, 161(1–2), 124–138.
- [14] L. Feng, Y. Zhang, J. Xi, Y. Zhu, N. Wang, F. Xia, L. Jiang, *Langmuir* **2008**, 24(8), 4114–4119.
- [15] M. K. Dawood, H. Zheng, T. H. Liew, K. C. Leong, Y. L. Foo, R. Rajagopalan, S. A. Khan, W. K. Choi, *Langmuir* **2011**, 27(7), 4126–4133.
- [16] S. Sethi, L. Ge, L. Ci, P. M. Ajayan, A. Dhinojwala, *Nano Letters* **2008**, 8(3), 822–825.
- [17] K. Liu, J. Du, J. Wu, L. Jiang, *Nanoscale* **2012**, 4(3), 768–772.
- [18] J. Li, X. Liu, Y. Ye, H. Zhou, J. Chen, *Colloids Surf., A* **2011**, 384(1–3), 109–114.
- [19] H. Chen, X. Zhang, P. Zhang, Z. Zhang, *Appl. Surf. Sci.* **2012**, 261(0), 628–632.
- [20] J. Genzer, K. Efimenko, *Science* **2000**, 290(5499), 2130–2133.
- [21] B. Li, J. Gao, X. Wang, C. Fan, H. Wang, X. Liu, *Appl. Surf. Sci.* **2014**, 290(0), 137–141.
- [22] C. Holtzinger, B. Niparte, S. Wächter, G. Berthomé, D. Riassetto, M. Langlet, *Surf. Sci.* **2013**, 617(0), 141–148.
- [23] S. M. Hurst, B. Farshchian, J. Choi, J. Kim, S. Park, *Colloids Surf., A* **2012**, 407(0), 85–90.
- [24] F. Liu, S. Wang, M. Zhang, M. Ma, C. Wang, J. Li, *Appl. Surf. Sci.* **2013**, 280(0), 686–692.
- [25] C. Wang, M. Zhang, Y. Xu, S. Wang, F. Liu, M. Ma, D. Zang, Z. Gao, *Adv. Powder Technol.* **2014**, 25(2), 530–535.
- [26] I. Bernagozzi, C. Antonini, F. Villa, M. Marengo, *Colloids Surf., A* **2014**, 441(0), 919–924.
- [27] W. Liu, Y. Luo, L. Sun, R. Wu, H. Jiang, Y. Liu, *Appl. Surf. Sci.* **2013**, 264(0), 872–878.
- [28] J. Song, Y. Lu, S. Huang, X. Liu, L. Wu, W. Xu, *Appl. Surf. Sci.* **2013**, 266(0), 445–450.
- [29] C. G. Obeso, M. P. Sousa, W. Song, M. A. Rodriguez-Pérez, B. Bhushan, J. F. Mano, *Colloids Surf., A* **2013**, 416(0), 51–55.
- [30] M. Joshi, A. Bhattacharyya, N. Agarwal, S. Parmar, *Bull Mater Sci* **2012**, 35(6), 933–938.
- [31] C.-H. Xue, J. Chen, W. Yin, S.-T. Jia, J.-Z. Ma, *Appl. Surf. Sci.* **2012**, 258(7), 2468–2472.
- [32] X. Zhou, Z. Zhang, X. Xu, X. Men, X. Zhu, *Appl. Surf. Sci.* **2013**, 276(0), 571–577.
- [33] Z. Shi, I. Wyman, G. Liu, H. Hu, H. Zou, J. Hu, *Polymer* **2013**, 54(23), 6406–6414.
- [34] I. Yilgor, S. Bilgin, M. Isik, E. Yilgor, *Polymer* **2012**, 53(6), 1180–1188.
- [35] W. Hou, Q. Wang, *Langmuir* **2009**, 25(12), 6875–6879.
- [36] M. Miyauchi, N. Kieda, S. Hishita, T. Mitsuhashi, A. Nakajima, T. Watanabe, K. Hashimoto, *Surf. Sci.* **2002**, 511(1–3), 401–407.
- [37] G. Caputo, C. Nobile, T. Kipp, L. Blasi, V. Grillo, E. Carlino, L. Manna, R. Cingolani, P. D. Cozzoli, A. Athanassiou, *J. Phys. Chem. C* **2008**, 112(3), 701.
- [38] R. Ramanathan, D. E. Weibel, *Appl. Surf. Sci.* **2012**, 258(20), 7950–7955.
- [39] R. Ramanathan, D. E. Weibel, *J. Braz. Chem. Soc.* **2013**, 24(6), 1041–1048.
- [40] C. B. Contreras, G. Chagas, M. C. Strumia, D. E. Weibel, *Appl. Surf. Sci.* **2014**, 307, 234–240.
- [41] R. Ramanathan, D. E. Weibel, *Appl. Surf. Sci.* **2012**, 258(20), 7950–7955.
- [42] A. Przyjazny, J. M. Kokosa, *J. Chromatogr. A* **2002**, 977(2), 143–153.
- [43] L. J. Bellamy, *The Infrared Spectra of Complex Molecules*, Chapman and Hall Ltd., London, UK **1975**, 299 pgs.
- [44] R. Ramanathan, D. E. J. Weibel, *Braz. Chem. Soc.* **2013**, 24(6), 1041–1048.